ACI STRUCTURAL JOURNAL TECHNICAL PAPER

Title no. 99-S12

Influence of Matrix Ductility on Tension-Stiffening Behavior of Steel Reinforced Engineered Cementitious Composites (ECC)

by Gregor Fischer and Victor C. Li

This paper investigates the interaction of structural steel reinforcement and high-performance fiber-reinforced cement composites (HPFRCC) in uniaxial tension. The effects of cementitious composite ductility on the steel reinforced composite deformation behavior are experimentally investigated and contrasted to conventional reinforced concrete. The substitution of brittle concrete with an engineered cementitious composite (ECC), which represents one particular type of HPFRCC with strain hardening and multiple cracking properties, has shown to provide improved load-deformation characteristics in terms of reinforced composite tensile strength, deformation mode, and energy absorption. Analysis of the deformation mechanisms suggests that the combination of steel reinforcement and ECC results in composite action, where unlike in reinforced concrete or conventional fiber-reinforced concrete (FRC), both constituent materials deform compatibly in the postcracking and postyielding deformation process. This deformation compatibility results in a more uniform strain distribution in reinforcement and composite matrix, reduced interfacial bond stress, and controlled damage at relatively large inelastic composite deformations. Research described in this paper particularly focuses on the influence of composite ductility on the deformation behavior of the reinforced composite and its effects on the strain distribution in the reinforcement, composite matrix, and interfacial bond.

Keywords: crack; ductility; reinforced concrete.

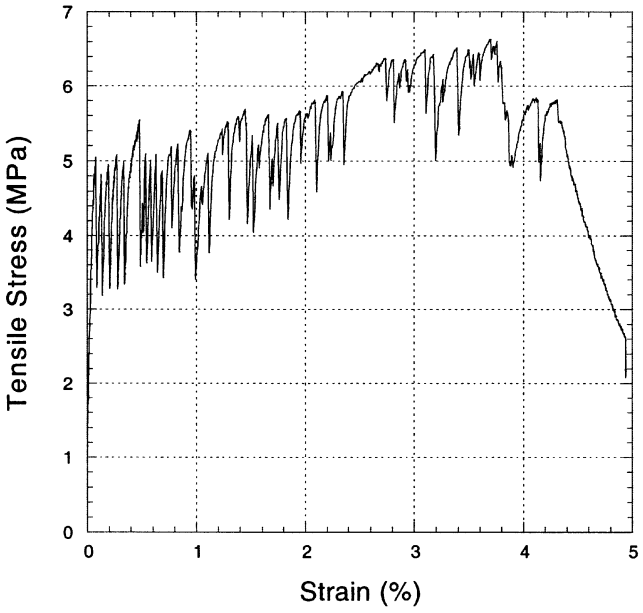

Fig. 1¾Tensile stress-strain relationship of ECC.

INTRODUCTION

The contribution of concrete to the load-deformation response of reinforced concrete (R/C) in uniaxial tension is generally described as the tension-stiffening effect (ACI Committee 224 1992). The response of the R/C composite is compared with that of the bare steel reinforcement, and the difference is attributed to the tensile stresses in the concrete matrix between transverse cracks. Due to the brittleness of concrete, these cracks cannot transfer any significant stress across the crack and, consequently, the maximum tensile load of the reinforced composite is limited by the tensile strength of the reinforcement, assuming minimum reinforcement is provided. Besides this limitation in load-carrying capacity, cracking of concrete causes a strain concentration in the steel reinforcement that the surrounding concrete is unable to accommodate. In addition, high bond stresses are required to transfer the tensile load into the concrete matrix between transverse cracks. Both phenomena result in the deterioration of the concrete matrix and adversely affect the intended composite mechanism.

To overcome this inherent weakness, the concrete matrix has been substituted with various fiber-reinforced cement matrices in a number of research studies in which the effect of increased tensile strength and toughness by steel fiber reinforcement of concrete has been investigated. For example, Abrishami and Mitchell (1997) reported that after cracking and significant deformation, plain concrete suffered splitting cracks and lost a significant amount of its stiffening contribution. The addition of steel fibers controlled the formation of these splitting cracks and resulted in improved tension stiffening behavior. Other studies similarly observed that high circumferential stresses lead to the development of longitudinal cracks, resulting in splitting and bursting of concrete cover (Krustulovic-Opara, Watson, and LaFave 1994). It has been found that the load level at which longitudinal cracking occurs is dependent on the cover thickness, the average bond stress at the interface, and the composite tensile stress-strain response. Furthermore, an increase in bond strength and bond stiffness has been attributed to the presence of steel fibers in the concrete.

In this study, an ECC with ductile deformation characteristics analogous to those of metals (Fig. 1) is used to emphasize the importance of the particular deformation characteristics of HPFRCCs. Previous research on the influence of fibers on the tension stiffening effect has primarily focused on the contribution of the fiber component to the postcracking strength gain of the reinforced composite

ACI Structural Journal, V. 99, No. 1, January-February 2002.
MS No. 01-065 received February 16, 2001, and reviewed under Institute publication policies. Pertinent discussion will be published in the November-December 2002 *ACI Structural Journal* if received by July 1, 2002.

Gregor Fischer *is a PhD student in the Department of Civil and Environmental Engineering at the University of Michigan, Ann Arbor. He received his MSE from the University of Michigan. His research interests include the design of fiber-reinforced cement composites and their structural applications.*

Victor C. Li *is a professor in the Department of Civil and Environmental Engineering at the University of Michigan. His research interests include micromechanics-based design of fiber-reinforced cementitious composites, and integrated materials-structural design for performance enhancement, including repair and retrofit of infrastructures.*

(Abrishami and Mitchell 1997; Noghabai 2000). In this study, the fiber-reinforced cement composite is treated as a composite material with elastic/plastic stress-strain characteristics. This approach is expected to appropriately capture the deformation mechanisms and interaction between reinforcement and the surrounding composite.

In this paper, for the sake of brevity, the authors refer to the steel reinforced concrete (R/C), steel reinforced FRC (R/FRC), and steel reinforced ECC (R/ECC) as structural composites, the steel reinforcing bar as the reinforcement, and the concrete, FRC, and ECC are generally referred to as the cementitious matrix (or simply the matrix).

The deformation characteristics of cementitious matrices are distinguished according to their postcracking deformation behavior (Naaman and Reinhardt 1995). Brittle matrices, such as concrete and plain mortar, lose their tensile load-carrying capacity almost immediately after formation of the first matrix crack. The addition of fibers in conventional FRC can increase the toughness of cementitious matrices significantly (Krustulovic-Opara, Watson, and LaFave 1994); however, their tensile strength beyond first cracking is not enhanced. FRC is therefore considered to be a quasibrittle material with tension-softening deformation behavior, that is, a decaying load and immediate localization of deformation at first cracking in the FRC matrix.

HPFRCCs are defined by an ultimate tensile strength higher than their first cracking strength and the formation of multiple cracking during the deformation process (Naaman and Reinhardt 1995). In contrast to localized deformation in FRC, where the apparent strain is dependent on the gage length, the deformation of HPFRCC is considered as a pseudo strain, which is a material property and independent of the gage length. The wording pseudo strain is used to distinguish the cracking-based deformation behavior in HPFRCC from the dislocation-based deformation mode in metals. A special version of HPFRCC, a micromechanically designed ECC (Li 1998), is used in the present study.

In this investigation, the R/ECC tensile member is treated as a composite consisting of a ductile matrix (ECC) reinforced with a ductile element (steel reinforcing bar). The combination of a ductile cementitious matrix with ductile reinforcement and their similar elastic-plastic deformation behavior is expected to result in improved load-deformation behavior in terms of composite tensile strength, deformation mode, and energy absorption. In addition to a reduced tendency of bond splitting due to confinement effect of fibers, the deformation compatibility between the ECC matrix and steel reinforcement on a macroscale is expected to lower bond stresses between the reinforcement and matrix. This particular phenomenon constitutes the most important distinction of R/ECC composites from R/C and R/FRC.

RESEARCH SIGNIFICANCE

The purpose of this paper is to investigate the influence of fiber-reinforced composite properties, particularly strain hardening and multiple cracking, on the tension stiffening effect of steel reinforced composite elements in uniaxial tension. The investigation focuses on the deformation mechanisms of the reinforced composite and the interaction between reinforcement and composite material with emphasis on the postcracking and postyielding regime. The significance of this research lies in the greatly improved performance of structural elements and systems made with R/ECC in terms of deformation compatibility between the reinforcement and ECC matrix, composite integrity at large deformations, damage tolerance, and repair needs. It is expected that the synergistic deformation behavior of steel reinforcement and strain-hardening ECC leads to enhanced structural behavior hitherto not achievable with tension-softening concrete or FRC. One class of structures expected to benefit from R/ECC elements is seismic-resistant structures, which require a relatively large inelastic deformation capacity. The new information obtained in this research provides a foundation for R/ECC structural design.

MATERIAL COMPOSITION AND PROPERTIES

The ECC matrix used in this particular study utilized 1.5% by volume of polyethylene fibers, cement, fine aggregates (average grain size 0.3 mm), water, high-range water-reducing admixtures, and admixtures to enhance the fresh properties of the mixture. Material properties obtained from this composition are a first cracking strength of 4.5 MPa at 0.01% strain and an ultimate tensile strength of 6.5 MPa at approximately 4% strain (Fig. 1). The tensile strain-hardening and the distributed microcracking behavior leading up to ultimate strength of ECC are useful indicators of the performance level of this HPFRCC. The compressive strength of this ECC matrix was 80 MPa.

Concrete utilized coarse aggregate (10 mm), cement, water, and a high-range water-reducing admixture to enhance the fresh properties. Tensile tests on concrete were not conducted, but are assumed to be the tensile first cracking strength of 4 MPa at 0.01% strain and subsequent brittle failure. The compressive strength of concrete used in this study was 50 MPa. The steel reinforcement in both specimen types had yield strength of 420 MPa at approximately 0.2% strain.

EXPERIMENTAL PROGRAM

Specimen configuration

In this study, two types of specimens were used to measure the overall load-deformation response and strain distribution in the steel reinforcement in the vicinity of a transverse crack (Type A) and along half-length of the tension-pull specimen (Type B).

Specimen Type A (Fig. 2(a)) had cross-sectional dimensions of 175 x 175 mm and length of 500 mm. To predetermine the location of first transverse cracking, a notch (a = 25 mm) was inserted at midspan of the specimen, and strain gages located inside the diametrically split reinforcing bar were placed adjacent to this particular position with a spacing of 15 mm to monitor the strain of the reinforcement during the deformation process. Additional strain gages were placed throughout the remaining half-length of the specimen at a spacing of 40 mm to observe the effect of transverse cracking on the uncracked part of the tension element. The reinforcement consisted of one steel reinforcing bar with a 25 mm diameter (No. 8 reinforcing

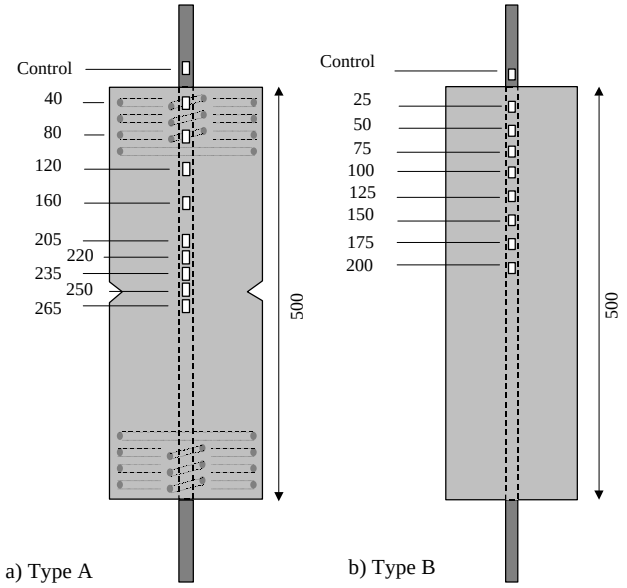

Fig. 2¾ Specimen configurations.

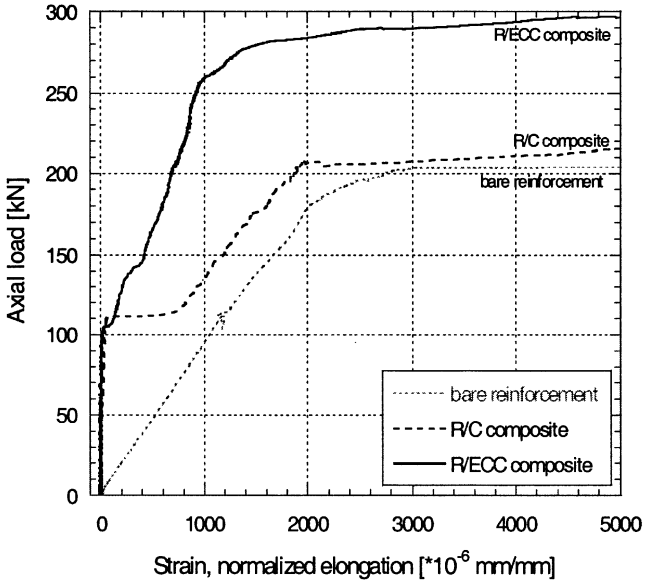

Fig. 3¾Load-deformation responses of specimens (Type A).

bar) that resulted in a reinforcement ratio of approximately 1.5% (the cavity in the reinforcing bar has been discounted). To prevent debonding between the reinforcing bar and composite matrix on both ends of the specimen due to the loading method (refer to description as follows), transverse reinforcement was provided over a length of 75 mm on each end.

Specimen Type B (Fig. 2(b)) had cross-sectional dimensions of 120 x 120 mm and length of 500 mm. Strain gages were mounted inside the diametrically split reinforcing bar with a spacing of 25 mm along half-length of the specimen. The reinforcement consisted of one steel reinforcing bar with a 19 mm diameter that resulted in a reinforcement ratio of approximately 1.8% (the cavity in the reinforcing bar has been discounted).

In both specimen types, the overall specimen deformation was measured by a pair of linear voltage differential transducers (LVDTs) on either side of the specimen mounted to the steel reinforcing bar close to the embedded portion of the specimen. The strain in the reinforcement outside the embedded segment was measured with a separate control strain gage.

The investigation of specimen Type A focused on the influence of matrix cracking on the strain distribution in the reinforcement in the immediate vicinity of a particular crack, while specimen Type B aimed at obtaining information on the effect of multiple cracking of ECC on the overall deformation behavior, especially beyond yielding of the steel reinforcement.

The R/C specimens were used as controls in analyzing the behavior of the R/ECC specimens.

Testing procedure

All specimens were installed in a servohydraulic testing machine and gripped at the protruding ends of the steel reinforcement so that the tensile load was transferred from the reinforcing bar to the specimen. Loading was applied under displacement control at a rate of 0.01mm/s.

For each specimen type (A and B), two specimens with concrete and two specimens with ECC matrix were tested, resulting in a total of eight specimens. All specimens remained in the formwork for 24 h after casting and were then wrapped and sealed (Type A) or water-cured (Type B) for 7 days. Testing was conducted at 28 to 35 days after casting.

Experimental observations

The load-deformation behavior of R/ECC and R/C for specimen Type A are described by comparing the respective reinforced composite response to the stress-strain behavior of the bare steel reinforcement (Fig. 3). For this purpose, the applied axial load is plotted versus the specimen elongation (from LVDT measurement) normalized by its initial length as well as strains measured by the control gages in the steel reinforcement.

In the initial loading stage prior to cracking of the matrix material, reinforcement and matrix deform elastically in R/C as well as in R/ECC. Transverse cracking in the matrix materials occurs when their first cracking strength is reached. Applied axial loads at this instance were 112 kN in R/C and 105 kN in R/ECC, suggesting that the first crack strengths of both matrices, concrete, and ECC are of similar value.

Transverse cracking occurred as expected in the region of reduced cross section (250 mm from loaded end) and resulted in a relatively large displacement increase (700 με) and a reduction in stiffness of the R/C specimen to a level approaching that of the steel reinforcement (Fig. 3). Further increasing specimen displacement was accommodated by a gradual increase of the transverse crack width. Yielding of the reinforced composite and bare reinforcement occurred simultaneously at an applied axial load of approximately 200 kN. Beyond yielding, the strain concentration in the reinforcing steel at the location of initial cracking causes radial pressure in the concrete matrix, resulting in the formation of a longitudinal splitting crack. Similar observations on the formation of longitudinal splitting cracks have been made in other studies (Tepfers 1979; Abrishami and Mitchell 1996; Noghabai 2000). Ultimately, further transverse cracking originated from the longitudinal splitting crack and also at 130 mm from the loaded end (Fig. 4(a)). Testing of R/C specimens was terminated due to composite disintegration when large parts of the concrete matrix detached from the reinforcement and major spalling occurred.

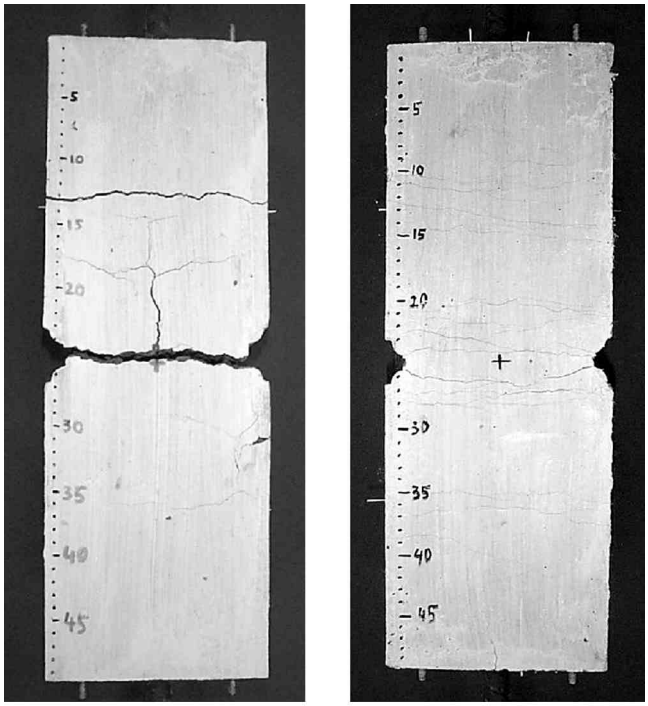

Fig. 4¾Crack patterns in specimens (Type A).

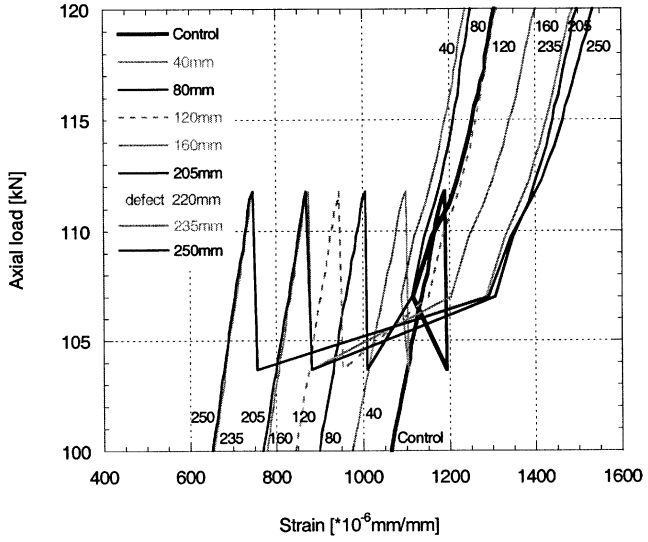

Fig. 5¾Local strains in reinforcement at cracking in R/C (Specimen Type A).

The different material characteristics of concrete and ECC become apparent at the formation of transverse cracking in the ECC matrix. At this instance, the load-deformation response of R/ECC specimen Type A (Fig. 3) showed a relatively small increase in elongation (100 με). The stiffness of the reinforced composite was subsequently reduced, but remained larger than that of the bare steel reinforcement. Increasing specimen displacement was accommodated by the formation of other transverse cracks, with individual crack widths stabilized at approximately 200 μm. Yielding of the reinforcement

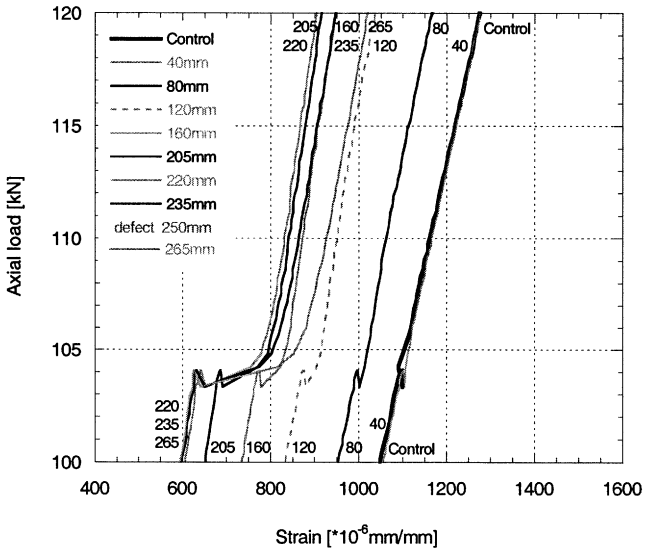

Fig. 6¾Local strains in reinforcement at cracking in R/ECC (Specimen Type A).

in the composite section of the specimen occurred at an axial load of 260 kN, while the bare reinforcement yielded at 200 kN. Failure of the R/ECC specimen was caused by necking and rupture of the protruding bare steel reinforcement at the loaded end of the specimen at an axial load of 310 kN. Except in the load transfer zone at both ends of the specimen, splitting cracks in the ECC matrix were not observed (Fig. 4(b)).

In specimen Type A, the local strain in the reinforcement in the vicinity of a transverse crack was of particular interest. The readings from the embedded strain gages inside the reinforcement show the local strain of the reinforcing bar at different positions in the specimen at the formation of the first transverse crack in the R/C (Fig. 5) and R/ECC (Fig. 6).

A number of observations can be made from these data in terms of strain distribution throughout the specimen prior to cracking, response of individual sections of the specimen to the formation of a transverse crack, and the impact of cracking on the interfacial bond in the vicinity of the crack.

Prior to cracking in R/C specimen Type A, local strains at individual sections of the reinforcement varied depending on the distance from the end of the specimen (Fig. 5). The transfer of applied axial load from the bare reinforcement to the concrete matrix is reflected in the gradual reduction of reinforcement strain with increasing distance from the end of the specimen. The obtained data does not give a clear indication of a termination of this transition zone, that is, where the axial load is fully shared between reinforcement and matrix and reinforcement strains become constant. This could be due to the short length of the specimen and relatively large diameter of the reinforcement or internal cracking of the concrete matrix. The formation of conical cracks originating from the ribs of the reinforcing steel can lead to an extension of the transition zone (Gastebled and May 2000). Only at midsection (235 and 250 mm) are the strains in the reinforcement constant, caused by specimen symmetry. The formation of the first transverse crack at a 112 kN axial load is coupled with a sudden load drop caused by elastically stored energy released at transverse cracking of the concrete matrix. Strain values at all sections of the specimen are affected by the subsequent redistribution of internal stresses in the composite. The control strain gage in the bare steel section as well as that at a

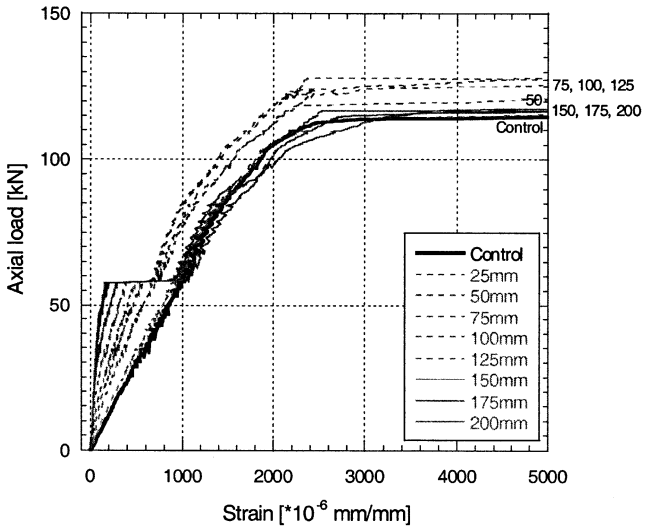

Fig. 7¾Strain distribution in R/C (Specimen Type B).

distance of 40 mm indicates a temporary contraction due to elastic unloading, while the section at the location of the transverse crack (250 and 235 mm) shows a severe increase in strain from 700 με before cracking to1400 με after cracking. Furthermore, gages at 205, 160, 120, and 80 mm also indicate strain jumps of different magnitudes. With further increasing axial load, local strain readings at 160, 205, 235, and 250 mm are larger than those of the bare steel reinforcement, which is unusual when considering axial load equilibrium. When comparing the apparent stiffness of individual sections of the reinforcement before and after cracking had occurred, it is observed that before cracking, the sectional stiffness increased with increasing distance from the specimen end. This reflects the gradual transfer of load from the reinforcement to the concrete matrix and composite action of both components. After the transverse crack had formed, strain gage readings from 250 to 160 mm indicate a reduction in sectional stiffness inversely proportional to the distance from the transverse crack.

In the R/ECC (Fig. 6) specimen, strain gages in the bare reinforcement and at a distance of 40 mm from the specimen end show equal strains despite the transverse reinforcement provided for confinement to prevent radial expansion of the matrix material in the load transfer zone. This could imply a lower bond stiffness of the ECC matrix compared with concrete, which is conceivable considering the lack of coarse aggregate in the ECC matrix. Transverse cracking occurs at an axial load of 104 kN. The strain gage in the bare steel and those at distances of 40 and 80 mm from the specimen end are virtually unaffected by the formation of the crack at specimen midsection. Similar symptoms in R/C, such as load drop and contraction of the bare reinforcement are observed, however, at a significantly smaller magnitude. The measured load drop in the R/ECC specimen was less than 1 kN compared with more than 8 kN in the R/C specimen. At the location of the crack, strain gages at 235 and 265 mm show a strain increase of 120 and 180 με respectively. With further increasing load, reinforcement strains at the location of the transverse crack remain smaller than that of the bare reinforcement due to the load-carrying contribution of the ECC matrix. The sectional stiffness at 265 and 235 mm is slightly reduced; however, all other sections of the specimen maintain their stiffness before and after formation of the crack.

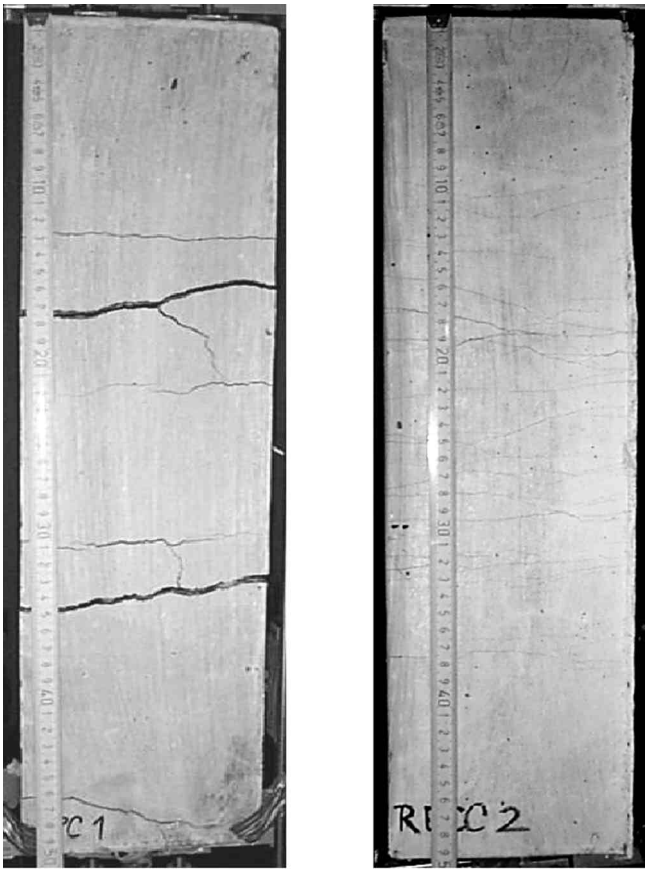

Fig. 8¾Crack patterns in specimens (Type B).

Specimen Type B (Fig. 2(b)) had a constant cross section, and cracking was expected to form randomly over the length of the specimen. Experimental observations from this specimen type were particularly focused on the strain distribution in the reinforcement in the postyielding regime.

In R/C specimen Type B (Fig. 7), transverse cracking occurred at an axial load of 65 kN at a distance of 170 mm from the specimen end. Strains at sections adjacent to the crack (150, 175, and 200 mm) rapidly increased and approached those of the bare reinforcement portion. These observations are similar to those made from R/C specimen Type A described previously. At increasing axial load and specimen displacement, yielding of the bare reinforcement and at the cracked location occurred simultaneously at a load of approximately 100 kN. A yield plateau was reached at 115 kN. Other sections of the specimen reached yield strain at higher axial load due to the contribution of uncracked concrete segments. Ultimately, additional transverse cracks formed at other locations along the specimen as well as splitting cracks (Fig. 8(a)), which further decreased the postyielding stiffness of the member (Fig. 9). The test was terminated when large portions of the concrete matrix detached from the reinforcement and major spalling occurred.

The R/ECC specimen Type B lacks a distinct first cracking load due to shrinkage-induced cracks formed prior to testing (Fig. 10). As was already observed in the R/ECC specimen (Type A), the overall load-deformation response indicates a significant contribution of the ECC matrix to the tensile strength of the reinforced composite, particularly in the postyielding regime (Fig. 11). Increasing axial displacement

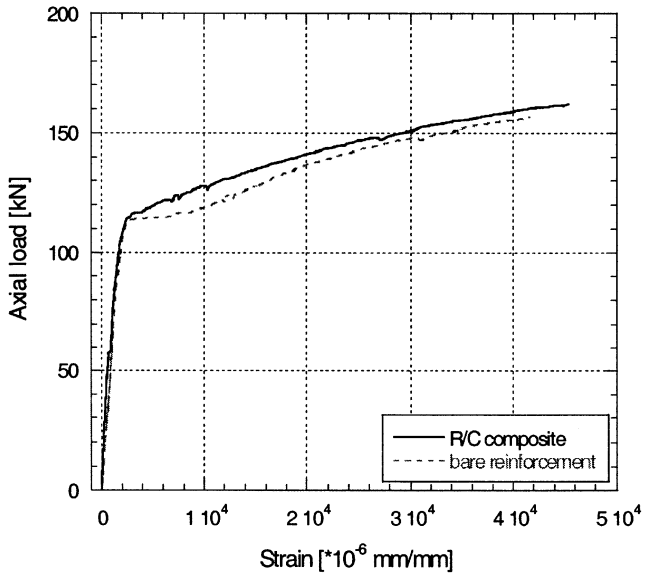

Fig. 9—Load-deformation response of R/C (Specimen Type B).

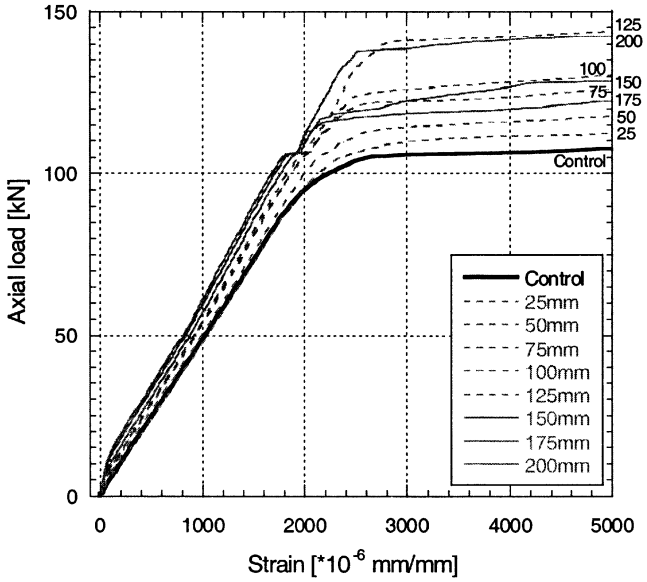

Fig. 10—Strain distribution in R/ECC (Specimen Type B).

was accommodated by the formation of multiple cracking in the ECC matrix. Approximately 40 transverse cracks with approximate crack widths of 200 μm and average crack spacing of 10 mm continuously develop along the specimen. At peak load (175 kN), the member reaches an average composite strain of 4% without localization of cracking (tension-softening) in the ECC matrix (Fig. 8(b)). This indicates that the ECC remains in the strain-hardening part of its stress-strain curve (Fig. 1) throughout the loading process. Prior to steel yielding, the strain readings show a decreasing strain in the reinforcement with increasing distance from the loaded end. At an axial load of 112 kN, the bare reinforcement reaches a yield plateau. At this load level, strain gages in the steel reinforcement at sections embedded in ECC matrix indicate the tendency to develop a yield plateau as well (Fig. 10); however, they further continue to deform elastically up to a point where yielding is finally reached (2000 to 2700 με). With the exception of sections at 150 and 175 mm, the strain distribution in the reinforcement indicates that yielding in the embedded portion of the specimen is further delayed as the distance from the specimen end increases. The test was terminated by necking and rupture of the bare steel section.

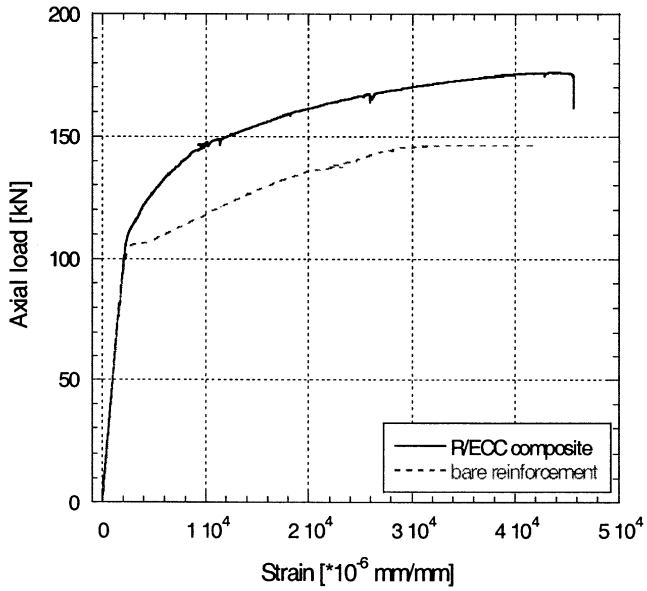

Fig. 11—Load-deformation response of R/ECC (Specimen Type B).

DISCUSSION

Prior to the formation of a transverse crack in specimen Type A, both matrices, concrete, and ECC provide similar contributions to the composite load-deformation behavior (Fig. 3). At this stage, the difference between a composite member and bare reinforcement response represents the tension-stiffening effect of the uncracked cementitious matrix. After cracking (112 kN in R/C and 104 kN in R/ECC), the comparison of the tensile load-deformation response of the R/C and R/ECC composite shows a more significant contribution of the ECC matrix as compared with concrete in terms of the tension-stiffening effect. Considering only the tensile strength of the reinforced composite, this effect is due to the load carried by the fibers in the matrix material and can be attributed to the tensile strength of the ECC matrix.

The characteristic deformation behavior of ECC, that is, formation of multiple cracking, has a more consequential effect on performance of the reinforced composite. Prior to reaching the first cracking strength of the cementitious matrix, the applied composite load is shared between the reinforcement and matrix proportional to their stiffness and volume fraction (Fig. 12(a)). Stresses in both components are uniformly distributed in sections beyond the load transfer zone of the specimen. The formation of a transverse crack in the R/C composite causes a redistribution of stresses in the matrix as well as in the reinforcement (Fig. 12(b)). Since the concrete matrix is not able to transfer stresses across the crack, the applied load must be transferred to the reinforcement by bond action (Abrishami and Mitchell 1996) and is entirely carried by the reinforcement at the crack location. Due to the stress concentration in the reinforcement and the stress-free concrete matrix at the crack location, both materials experience a relatively large strain difference that results in bond stresses and local slip. Consequently, composite deterioration can occur in various scenarios, such as interfacial bond failure, formation of inclined cracks originating from the interface,

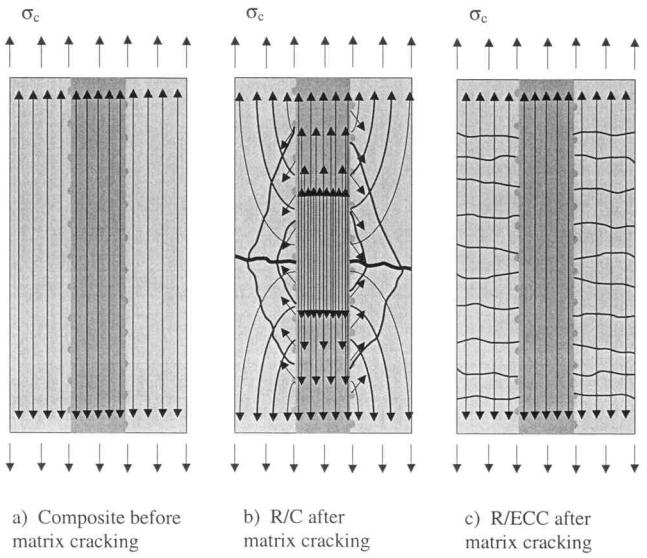

Fig. 12¾Schematic of crack formation and internal stresses in R/C and R/ECC composite.

and longitudinal splitting due to radial pressure (Goto 1971) exerted by the ribs of the deformed reinforcing bar on the surrounding concrete.

The multiple cracking property of the ECC matrix can, on a macroscale, eliminate the strain difference between reinforcement and matrix material. The R/ECC member may be considered as a composite of two materials having an elastic/plastic deformation behavior with individual yield strength and strain. Cracking of ECC represents yielding of the matrix component while the steel reinforcement remains elastic. After cracking, the stress distribution in the R/ECC composite is virtually unchanged (Fig. 12(c)) since the stress in the ECC matrix at this instance remains constant and further increases with increasing deformation. In essence, the tensile stress in the matrix carried prior to cracking is directly transferred (via bridging fibers) back to the uncracked parts of the matrix once the crack has formed. On a macroscale, bond stresses are not required to facilitate this transfer since load carried by the ECC matrix need not be transferred to the reinforcement. Due to the uniform stress in the cracked matrix, the distance between transverse cracks is a function of material properties of the fiber-reinforced cement composite (ECC) and is independent of the interfacial bond properties between reinforcement and matrix. Considering local effects in the immediate vicinity of one discrete crack in the ECC matrix, however, some interaction between reinforcement and matrix is expected. Depending on the micromechanical properties of the ECC matrix, a certain crack opening is required to develop a fiber bridging stress equal to that of the composite prior to cracking. Due to this microscopic discontinuity, localized interfacial bond between steel reinforcement and ECC matrix is activated.

Yielding of the steel component constitutes the final deformation stage of the R/ECC member, where both constituent materials have entered the inelastic deformation regime. Strain-hardening deformation behavior of both components (steel and ECC) prevents the localization of deformation at a particular section. Cracking of ECC as well as yielding of reinforcement is distributed over the length of the specimen. Because of the large volume of material involved in the inelastic deformation process, energy absorption is significantly enhanced. The fact that the ECC contribution to the load-carrying capacity can be maintained at relatively large deformation levels beyond steel yielding is directly attributed to the ductility of the ECC matrix, that is, the multiple cracking deformation behavior.

Evidence for these suggested mechanisms is partly provided by the strain gage readings from both specimen types for the stress distribution in the reinforcement at first cracking (Type A) as well as beyond yielding (Type B).

At formation of a transverse crack in R/C specimen Type A (Fig. 5), tensile stress in the matrix is released (load drop) and transferred to the reinforcing bar, which results in a rapid strain increase at the cracked section (250 mm). Other sections (235 and 205mm) simultaneously show a strain increase up to the same value (1400 με), suggesting that the concrete matrix at these locations is not contributing to the sectional response due to debonding or internal matrix cracking. The fact that reinforcement strain readings at sections between 250 and 160 mm are larger than that of the bare reinforcement may be influenced by a stress concentration at the location of the transverse crack (acting like a ring crack with crack front impinging on the steel bar) and the effect of concrete confinement on the deformation mode of the steel reinforcement.

In R/ECC specimen Type A (Fig. 6), the load drop at cracking is less severe than in R/C since at cracking the tensile stress in the matrix is transferred through the fibers in the ECC matrix. The opening of the transverse crack is accommodated by the steel reinforcement, and sections in the immediate vicinity of the transverse crack experience a strain increase. This increase is of small magnitude compared with R/C due to the smaller crack opening in R/ECC. Strains at all sections remain well below that of the bare reinforcement, indicating that despite the presence of a crack, the matrix not only stiffens the reinforced composite in the uncracked sections but also actively contributes to the axial load-carrying capacity at the cracked section. This results in an improved tensile response of R/ECC compared with R/C (Fig. 3), where, beyond cracking, the composite stiffness and load-deformation response is governed by the reinforcement while the uncracked concrete matrix merely restrains parts of the steel reinforcement from deforming.

The effect of pseudo-strain hardening and multiple cracking on the deformation characteristics of the reinforced composite becomes apparent at specimen displacements beyond first cracking and particularly beyond yielding of the reinforcement.

The strain distribution in the reinforcement of R/C specimen Type B (Fig. 7) shows that the strains in the bare reinforcement and at the location of the transverse crack are identical. Consequently, the load-deformation response of the composite (Fig. 9) indicates only a minor difference between bare reinforcement and composite behavior beyond yielding of the reinforcement. This stiffening effect is due to a larger reinforcement strain at the cracked section compared with the bare reinforcement and strain-hardening behavior of steel. The strain difference between reinforcement and stress-free matrix at the cracked section results in local slip and circumferential stress in the concrete matrix that leads to deterioration of interfacial bond and longitudinal splitting cracks.

Prior to yielding of R/ECC specimen Type B, a number of transverse cracks had formed throughout the specimen while the steel reinforcement remained elastic. Yielding of the bare reinforcement initiates yielding in other sections as well (Fig. 10); however, as a strain of approximately 2000 με is reached, the ECC matrix picks up part of the axial load and

delays yielding of reinforcement in these sections as they temporarily continue to deform elastically. Increasing specimen displacement is simultaneously accommodated by increasing strain in reinforcement as well as in the ECC matrix, preventing local slip by axial deformation compatibility. At this stage, both components of the reinforced composite experience inelastic deformation with increasing tensile stress due to strain-hardening behavior. The composite maintains its integrity at these relatively large inelastic deformation levels without localization of deformation and subsequent damage, such as longitudinal splitting cracks or spalling of matrix material (Fig. 8).

CONCLUSIONS

The comparison of R/C and R/ECC has shown qualitative and quantitative differences in their tension-stiffening behaviors. The combination of reinforcement and matrix material with elastic/plastic stress-strain behavior results in a composite where both materials are deforming compatibly in the inelastic deformation regime. Consequently, damage induced by local slip and excessive interfacial bond stress between reinforcement and matrix is prevented. The ECC matrix stiffens the specimen at uncracked sections and also strengthens it at cracked sections. Hence, the composite load-deformation response is significantly improved in terms of axial load-carrying capacity as well as ductility. To maintain this composite action at relatively large inelastic deformations, strain hardening and multiple cracking of the ECC matrix are essential. It should be emphasized that the resulting composite behavior is not primarily achieved by enhanced material resistance in terms of matrix tensile strength, confinement effect, or interfacial bond strength, but rather by reducing internal stresses that would necessitate such resistance. Compatible deformation between ECC and steel reinforcement implies that bond strength in R/ECC is not as significant as in R/C for enhanced structural performance.

ACKNOWLEDGMENTS

The research described in this paper has been supported by a grant from the National Science Foundation to the ACE-MRL at the University of Michigan. This support is gratefully acknowledged.

REFERENCES

Abrishami, H. H., and Mitchell, D., 1996, "Influence of Splitting Cracks on Tension Stiffening," *ACI Structural Journal*, V. 93, No. 6, Nov.-Dec., pp. 703-710.

Abrishami, H. H., and Mitchell, D., 1997, "Influence of Steel Fibers on Tension Stiffening," *ACI Structural Journal*, V. 94, No. 6, Nov.-Dec., pp. 769-776.

ACI Committee 224, 1992, "Cracking of Concrete Members in Direct Tension (ACI 224.2R-92)," American Concrete Institute, Farmington Hills, Mich., 12 pp.

Gastebled, O. J., and May, I. M., 2000, "Numerical Simulation of Pulled Specimens," *ACI Structural Journal*, V. 97, No. 2, Mar.-Apr., pp. 308-315.

Goto, Y., 1971, "Cracks Formed in Concrete Around Deformed Tension Bars," ACI JOURNAL, *Proceedings* V. 68, No. 4, Apr., pp. 244-251.

Krstulovic-Opara, N.; Watson, K. A.; and LaFave, J. M., 1994, "Effect of Increased Tensile Strength and Toughness on Reinforcing-Bar Bond Behavior," *Cement & Concrete Composites*, V. 16, pp. 129-141.

Li, V. C., 1998, "Engineered Cementitious Composites—Tailored Composites through Micromechanical Modeling," *Fiber Reinforced Concrete: Present and the Future*, N. Banthia, A. Bentur, and A. Mufti, eds., Canadian Society for Civil Engineering, Montreal, pp. 64-97.

Naaman, A. E., and Reinhardt, H. W., 1995, "Characterization of High-Performance Fiber Reinforced Cement Composites—HPFRCC," *Proceedings of High-Performance Fiber Reinforced Cement Composites 2 (HPFRCC 2)*, A. E. Naaman and H.W. Reinhardt, eds., pp. 1-23.

Noghabai, K., 2000, "Behavior of Tie Elements of Plain and Fibrous Concrete and Varying Cross Sections," *ACI Structural Journal*, V. 97, No. 2, Mar.-Apr., pp. 277-284.

Tepfers, R., 1979, "Cracking of Concrete Cover along Anchored Deformed Reinforcing Bars," *Magazine of Concrete Research*, V. 31, No. 106, Mar., pp. 3-12.